The ephemeral and elusive ocean carbon response to COVID-related emissions reductions

Nicole S. Lovenduski[1], Neil C. Swart[2], Adrienne J. Sutton[3], John C. Fyfe[2], Galen A. McKinley[4], Christopher Sabine[5], Nancy L. Williams[6]

[1]Department of Atmospheric and Oceanic Sciences and Institute of Arctic and Alpine Research, University of Colorado, Boulder, CO, USA
[2]Canadian Centre for Climate Modelling and Analysis, Environment and Climate Change Canada, Victoria, BC, Canada
[3]Pacific Marine Environmental Laboratory, National Oceanic And Atmospheric Administration, Seattle, WA, USA
[4]Columbia University and Lamont Doherty Earth Observatory, Palisades, NY, USA
[5]Department of Oceanography, University of Hawai'i at Manoa, Honolulu, HI, USA
[6]College of Marine Science, University of South Florida, St. Petersburg, FL, USA

Key Points:

- COVID-related emissions reductions will be imperceptible in surface ocean pH observations
- The CanESM5 COVID ensemble predicts a unique fingerprint of COVID-related emissions reductions in global mean ΔpCO_2 (pCO_2^{oc} - pCO_2^{atm})
- The fingerprint is potentially detectable in global-scale observations of ΔpCO_2, but only with large emissions reductions

Corresponding author: Nicole S. Lovenduski, nicole.lovenduski@colorado.edu

Abstract

The decline in global emissions of carbon dioxide due to the COVID-19 pandemic provides a unique opportunity to investigate the sensitivity of the global carbon cycle and climate system to emissions reductions. Recent efforts to study the response to these emissions declines has not addressed their impact on the ocean, yet ocean carbon absorption is particularly susceptible to changing atmospheric carbon concentrations. Here, we use ensembles of simulations conducted with an Earth system model to explore the potential detection of COVID-related emissions reductions in the partial pressure difference in carbon dioxide between the surface ocean and overlying atmosphere (ΔpCO_2), a quantity that is regularly measured. We find a unique fingerprint in global-scale ΔpCO_2 that is attributable to COVID and potentially detectable in observations, but only with much larger emissions reductions than those that have been observed to date.

Plain Language Summary

The COVID-19 pandemic is slowing the rate of fossil fuel use, and thus slowing the rise of carbon dioxide in the atmosphere. Here we explore what this change in fossil fuel use does to carbon in the ocean. We use a climate model to estimate the change in ocean-atmosphere carbon exchange and ocean acidity. Since we don't yet know how much we will slow our fossil fuel use due to COVID, we make several guesses and see how our model ocean responds to each. We use the model to investigate whether the change that we model would be detectable in the real world observations. We find that it is nearly impossible to detect a COVID-related change in ocean acidity with observations. It might be possible to detect a COVID-related change in ocean-atmosphere carbon exchange, but only if we drastically slow our emissions, and only if we have enough observation stations in place to record it.

1 Introduction

The socioeconomic disruptions associated with the COVID-19 pandemic have caused an unprecedented drop in global emissions of carbon dioxide (CO_2) and other atmospheric pollutants. The first half of 2020 was characterized by an 8.8% decrease in global CO_2 emissions relative to the first half of the previous year [*Liu et al.*, 2020], with average daily emissions declines peaking at -26% in individual countries [*Le Quéré et al.*, 2020]. The duration and severity of the emissions decline in the latter half of 2020 and beyond is as yet unknown, but 2020 emissions are likely to change by -6% to -13% [*Friedlingstein et al.*, 2020] and continued CO_2 emissions reductions are expected in 2021 [*Liu et al.*, 2020]. The important role of CO_2 emissions in the global carbon cycle and climate system motivates further research on this topic.

Several research groups are actively studying the impact of the COVID-related emissions reductions on the atmosphere and climate system. The latest World Meteorological Organization bulletin reports slight reductions in 2020 atmospheric CO_2 levels (-0.08 to -0.23 ppm) as a result of the COVID pandemic, though they emphasize that this reduction is difficult to detect given typical year-to-year variations in atmospheric CO_2 [$\pm$ 1 ppm; *World Meteorological Organization*, 2020]. A recent modeling study concurs that COVID-related reductions in atmospheric CO_2 levels are likely undetectable unless the emissions reductions are substantially larger than observed, but also demonstrates that these short-term reductions will have a long-term (decadal or longer) influence on atmospheric CO_2 concentrations due to the long-lived nature of CO_2 in the atmosphere [*Fyfe et al.*, 2020]. Modeling studies suggest a modest or negligible impact of the emissions reductions on global atmospheric temperature [*Forster et al.*, 2020; *Fyfe et al.*, 2020]. To date, no study has described the impact of COVID-related emissions reductions on the ocean. As the ocean carbon system is particularly susceptible to atmospheric CO_2 levels, further study on this topic is warranted.

Previous modeling work implies that the COVID-related CO_2 emissions reductions and the subsequent slowdown in the atmospheric CO_2 growth rate will have an immediate impact on ocean carbon uptake. Using an upper ocean box model that solves for the time rate of change of dissolved inorganic carbon in the surface mixed layer, *McKinley et al.* [2020] showed high sensitivity of air-sea CO_2 flux to slight variations in the growth rate of the atmospheric partial pressure of CO_2 (pCO_2^{atm}) over the 1990s and 2000s. Using a global Earth system model, *Laughner et al.* [in review] find an anomalous 70 Tg C yr^{-1} reduction in 2020 sea-to-air CO_2 flux due to COVID. These findings prompt further investigation into the detection of COVID-related CO_2 emissions reductions in ocean carbon observations.

Here, we explore the potential to detect COVID-related CO_2 emissions reductions in two measurable quantities for ocean carbon: (1) ΔpCO_2, which is the difference between the partial pressure of CO_2 in the surface ocean (pCO_2^{oc}) and the overlying pCO_2^{atm} and determines the direction and, along with wind speed and solubility, the magnitude of the sea-to-air CO_2 flux, and (2) surface ocean pH, a measure of ocean acidity. Using ensembles of simulations conducted with a single Earth system model, we identify the fingerprint of COVID-related CO_2 emissions reductions in these observable quantities. We then treat the individual model ensemble members as possible observations and remark on the likelihood of fingerprint detection in future ocean carbon measurements.

2 Methods

2.1 CanESM5 COVID ensemble

Our primary numerical tool is the Canadian Earth System Model version 5 (CanESM5), which consists of coupled atmosphere, ocean/sea ice, and land model components and was designed to make estimates of historical climate change and variability, to provide future climate projections, and to initialize near-term predictions of the climate system [*Swart et al.*, 2019]. The ocean component of the model is based on the Nucleus for European Modelling of the Ocean (NEMO), but has been configured for use in CanESM5 with a nominal 1° horizontal resolution that refines to 1/3° meridional grid spacing near the equator, 45 vertical layers with varying thickness from 6 m in the surface to 250 m at depth, and a collection of scientifically supported sub-grid scale mixing schemes [*Swart et al.*, 2019]. The ocean biogeochemical component of the model uses the Canadian Model for Ocean Carbon [CMOC; *Christian et al.*, 2010], a Nutrient, Phytoplankton, Zooplankton, Detritus (NPZD)-type biological model with updated carbonate chemistry routines following the Ocean Model Intercomparison Project biogeochemical (OMIP-BGC) protocol [*Orr et al.*, 2017].

We analyze output from a large ensemble of CanESM5 simulations forced with 4 different CO_2 emission scenarios (Figure 1a). This model simulation configuration is described in *Fyfe et al.* [2020], and hereafter referred to as the CanESM5 COVID ensemble. Briefly, the first set of simulations (the control) consists of 30 ensemble members of CanESM5 integrated over 2015-2019 under SSP2-4.5 CO_2 emissions and initialized with slightly perturbed climate states to capture internal climate variability. The remaining 3 ensembles follow the same initialization procedure with 30 ensemble members each over 2019-2040, but are forced with a COVID-like CO_2 emissions reduction that begins in December 2019 and resolves by December 2021 (Figure 1a). Peak emissions reductions of 25% (COVID-like), 50% (2 × COVID-like), and 100% (4 × COVID-like) occur in May 2020 (Figure 1); these scenarios correspond to 2020 annualized emissions reductions of 16%, 32%, and 63%, respectively [*Fyfe et al.*, 2020].

CanESM5 is an appropriate tool for the exploration of the ocean carbon response to COVID-related emissions reductions. A previous evaluation of the CMIP6 historical simulation of CanESM5 via comparison with historical climatologies finds high spatial correlation ($r > 0.9$) of modeled and observed three-dimensional potential temperature, nitrate, oxygen, and dissolved inorganic carbon [*Swart et al.*, 2019]. However, the same study finds lower

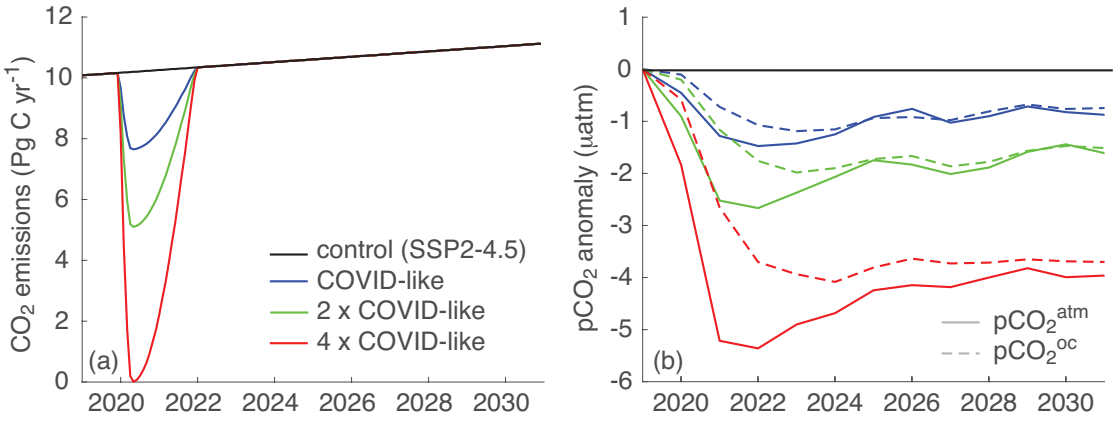

Figure 1. (a) Global-mean CO_2 emissions (Pg C yr^{-1}) for the (black) control/SSP2-4.5, (blue) COVID-like, (green) 2 × COVID-like, and (red) 4 × COVID-like scenarios. (b) Global-, annual-, and ensemble-mean surface (solid) pCO_2^{atm} and (dashed) pCO_2^{oc} anomaly (μatm; difference from control) simulated in the CanESM5 ensembles under the COVID-like emission scenarios. Adapted from *Fyfe et al.* [2020].

spatial correlations (r = 0.7) between modeled and observation-based historical air-sea CO_2 flux [*Swart et al.*, 2019], prompting our further evaluation of ocean observables ΔpCO_2 and surface ocean pH over the historical period. Figure **??**a illustrates similar spatial patterns of annual-mean ΔpCO_2 across the global ocean between the CanESM5 control ensemble mean and version 2020 of the *Landschützer et al.* [2016] observation-based climatology [*Landschützer et al.*, 2020] over 2015-2018, though we note regional differences in the magnitude and spatial extent of positive ΔpCO_2 across the equatorial Pacific, in the sign of ΔpCO_2 in the subtropical North Atlantic, and in the spatial extent of the positive ΔpCO_2 region in the eastern subtropical North Pacific. We also note a lack of observation-based estimates of ΔpCO_2 in the Arctic, where CanESM5 predicts large negative ΔpCO_2 values (Figure **??**a,b). The CanESM5 control ensemble is capable of capturing the phasing and magnitude in the climatological seasonal cycle of ΔpCO_2 as measured at the the Woods Hole Oceanographic Institution Hawaii Ocean Timeseries Site (WHOTS) buoy, though the spring minimum is deeper in approximately half of the CanESM ensemble members than observed (Figure **??**b). While the annual mean surface ocean pH over 2015-2018 exhibits similar spatial patterns between modeled pH and an observation-based product [*Gregor and Gruber*, 2020], the modeled pH is generally lower than that from observation-based estimates (Figure **??**). As with ΔpCO_2, a lack of observation-based climatological estimates of pH in the seasonally ice covered Southern Ocean and Arctic precludes investigation of model-observation similarity in these regions. CanESM5 produces rates of historical ocean carbon uptake that are consistent with observational estimates of decadal mean CO_2 fluxes and with independent estimates of cumulative anthropogenic carbon uptake at the global scale [*Swart et al.*, 2019], suggesting that the simulated response of ocean carbon to atmospheric CO_2 changes is reliable at the large scale.

2.2 Statistical approach

We identify the COVID-related fingerprints in ΔpCO_2 and pH using CanESM5 COVID ensemble mean output that has been annually and globally averaged over 2019-2024. This 5-year period captures the time during which we observe the largest anomalies in atmospheric and oceanic pCO_2 relative to the control ensemble across each of the COVID emissions scenarios (see also Figure 1b). We identify the fingerprint using ensemble and global-mean output to maximize the influence of external forcing and dampen the influence of internal vari-

ability on the fingerprint [*Lovenduski et al.*, 2016; *McKinley et al.*, 2016; *Schlunegger et al.*, 2019, 2020]. The spatial pattern associated with the COVID-related fingerprint is estimated as the regression coefficient of the ensemble mean at each location and the standardized fingerprint (subtract mean and divide by standard deviation) over 2019-2024 for each emission scenario.

Detection and attribution of the COVID signal is assessed by analyzing the set of 30 Pearson's correlation coefficients (r) produced when correlating individual ensemble members with the corresponding fingerprint over 2019-2024. The statistical properties (mean, standard deviation) of these coefficients are estimated via Fisher z-transformation.

3 Results

The CanESM5 COVID ensemble predicts an anomalous decrease in surface pCO_2^{atm} and pCO_2^{oc} due to the CO_2 emissions reduction, as evidenced by the negative anomalies in annual mean, ensemble mean pCO_2^{atm} and pCO_2^{oc} calculated relative to the control/SSP2-4.5 emissions scenario (Figure 1b). Anomalously low pCO_2^{atm} peaks in 2021-2, approximately 1-2 years after the largest emissions reduction, reflecting the mixing time of CO_2 in the global atmosphere. At their peak, global mean anomalies in pCO_2^{atm} are -1.5, -2.7, and -5.4 μatm for the COVID-like, 2× COVID-like, and 4× COVID-like emission scenarios, respectively. Anomalously low pCO_2^{oc} peaks in 2023-4, approximately 1-2 years after the largest pCO_2^{atm} reduction, reflecting the equilibration timescale of the surface ocean mixed layer with atmospheric CO_2 perturbations [*McKinley et al.*, 2020]. At their peak, global mean anomalies in pCO_2^{oc} are smaller in magnitude than the pCO_2^{atm} anomalies for the corresponding emission scenario (-1.2, -1.9, and -4.1 μatm for the COVID-like, 2× COVID-like, and 4× COVID-like emission scenarios, respectively). Unlike the CO_2 emissions anomalies (Figure 1a), the pCO_2^{atm} and pCO_2^{oc} anomalies persist for the duration of the simulations (Figure 1b), due to the long-lived nature of CO_2 in the atmosphere [*Fyfe et al.*, 2020].

The difference between the evolution of pCO_2^{atm} and pCO_2^{oc} following the COVID-like CO_2 emissions reductions creates a unique fingerprint in ΔpCO_2 across the CanESM5 COVID ensemble (Figure 2a-c). Figure 2 (top row) shows the evolution of the annual mean, global mean ΔpCO_2 from the 30 individual ensemble members (light gray) and the ensemble mean (black) across the three COVID scenarios. The fingerprint for each scenario is indicated as the colored part of the ensemble mean ΔpCO_2, capturing the temporal behavior over 2019-2024 (Figure 2a-c). This fingerprint is characterized by an increase in ΔpCO_2 from 2019 to 2021, followed by a decrease over 2021-2024, and is most pronounced in the 4 × COVID-like case and least pronounced in the COVID-like case. This inverted "V" fingerprint/time-series is unique; it arises due to the rapid slowdown and recovery of CO_2 emissions and the ~1 year equilibration timescale for carbon between the atmosphere and the ocean mixed layer [Figure 1b; *McKinley et al.*, 2020]. In contrast, a typical year-on-year emissions reduction scenario – for example, a scenario that limits warming to 1.5°C – generates a slowly-changing ΔpCO_2 whose fingerprint would be challenging to distinguish (not shown).

The evolution of ocean acidification under COVID-like emissions reductions produces an almost imperceptible fingerprint in global mean surface ocean pH. Here, the large and long-lived anthropogenic CO_2 burden in the atmosphere drives continued ocean carbon uptake and thus decreasing global pH relative to the base period in all ensemble members over 2019-2040 (Figure 2d-f). The rate of pH decrease briefly stagnates under COVID-like emissions reductions, with the biggest stagnation under the 4 × COVID-like emissions scenario (Figure 2f). This fingerprint in surface ocean pH would be difficult to distinguish in the observational record due to large measurement uncertainty relative to the projected rate of pH decrease. Thus, for the remainder of our study, we focus our analysis efforts on the unique ΔpCO_2 fingerprint brought about by COVID-related emissions reductions.

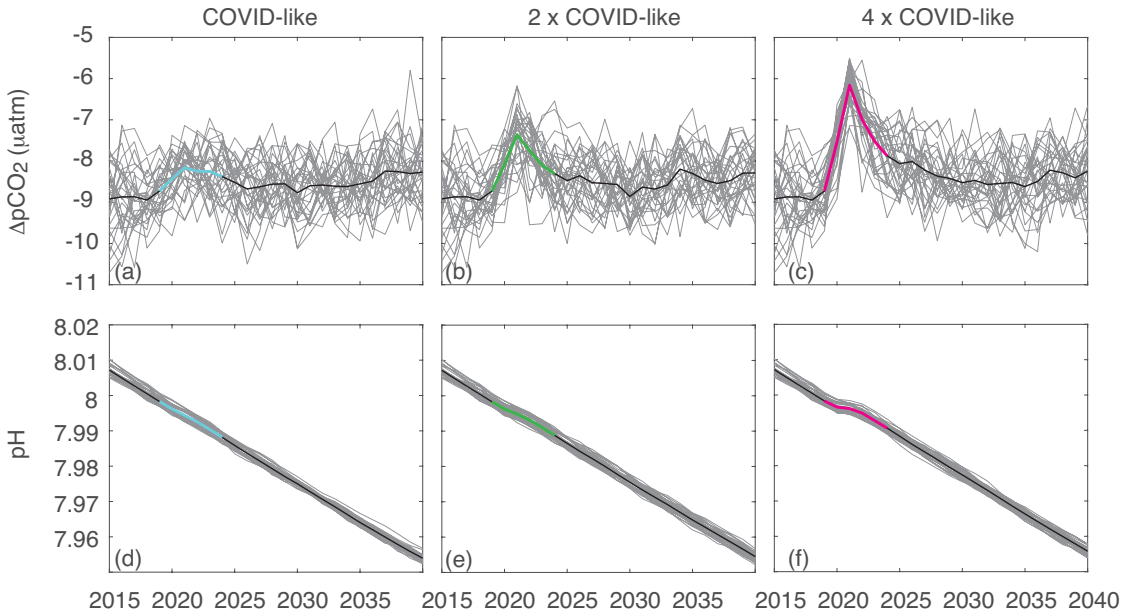

Figure 2. COVID-related fingerprints in global-mean, annual-mean (top row) ΔpCO_2 (pCO_2^{oc}-pCO_2^{atm}; μatm) and (bottom row) surface ocean pH, simulated with the CanESM5 COVID ensemble. Gray lines show individual ensemble members, black line shows the ensemble mean, and colored lines show the COVID-related fingerprint over 2019-2024 under the (first column) COVID-like, (second column) 2 × COVID-like, and (third column) 4 × COVID-like emission scenarios.

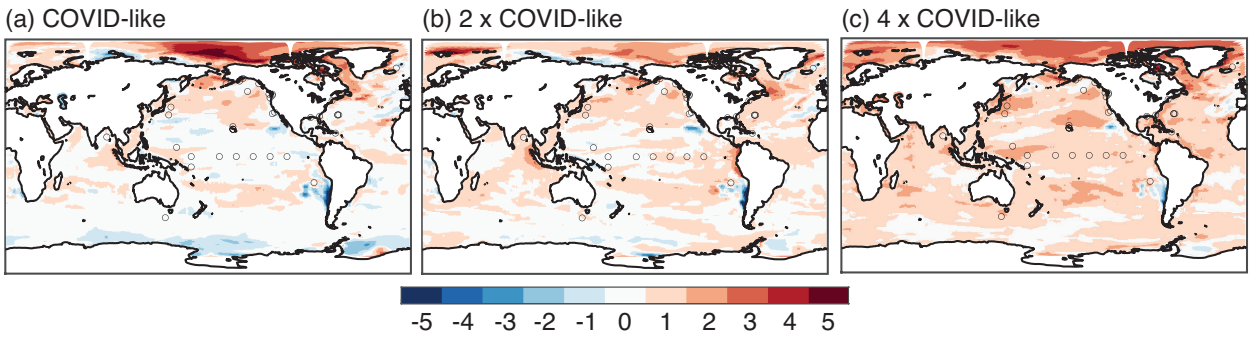

Figure 3. Spatial pattern of the COVID-related fingerprints in ΔpCO_2 (pCO_2^{oc}-pCO_2^{atm}; μatm) under the (a) COVID-like, (b) 2 × COVID-like, and (c) 4 × COVID-like emission scenarios, calculated as the regression coefficient of ΔpCO_2 onto the standardized fingerprints. Black open circles indicate the locations of buoys capable of autonomous surface ocean pCO_2 measurements from *Sutton et al.* [2019].

The COVID-related fingerprints in ΔpCO_2 are characterized by a heterogeneous spatial pattern across the CanESM5 global ocean. Figure 3 shows the magnitude of the fingerprint signal at each location. The largest fingerprint signals (> 2 μatm) manifest in the Arctic Ocean, the subtropical North Pacific, and the western subpolar North Atlantic (Figure 3). The fingerprint signals become more widespread with larger emissions reductions, such that a majority of the global ocean experiences a fingerprint signal in the $4 \times$ COVID-like emissions scenario (Figure 3c).

Is it possible to detect our modeled ΔpCO_2 fingerprint in the real ocean, and to attribute the fingerprint to COVID-related emissions reductions? To answer this question, we treat the individual CanESM5 COVID ensemble members as equally likely observations of the recent past / near future and examine their correlation to the ensemble mean. Figure 4a shows the range of correlation coefficients across the 30 ensemble members under the four emission scenarios for the global mean ΔpCO_2. The mean correlation coefficient is near zero for the control simulation (not exactly zero due to the long term trend in ΔpCO_2 under SSP2-4.5), with a wide range; COVID-like emissions reductions increase the mean and narrow the range, supporting the attribution of the ΔpCO_2 signal to COVID. There is enhanced likelihood of detection of the COVID signal from global-mean ΔpCO_2 observations with more severe reductions in emissions, as evidenced by the increasing mean correlation coefficient with larger emissions reductions. However, the range of correlation coefficients is only statistically different from zero (using the $\pm 1\sigma$ or 67% confidence interval) in the $4 \times$ COVID-like scenario. Thus, while the evolution of the global mean ΔpCO_2 anomaly is potentially detectable in observations and attributable to COVID emissions, a much larger emissions reduction than observed to date would be required to truly detect the signal in the real ocean.

It is nearly impossible to detect the COVID-related fingerprint in ΔpCO_2 at a single observational site due to high local internal variability and measurement uncertainty. Figure 3 shows the location of buoys capable of near real-time autonomous surface ocean pCO_2 measurements (< 2 μatm uncertainty) as open black circles; these 40 observational buoys are discussed in detail in *Sutton et al.* [2019]. Both a strong signal (COVID fingerprint) and low noise (internal variability) are required for detection at a single site. In all emission scenarios, the CanESM5 COVID ensemble predicts the strongest ΔpCO_2 fingerprint signals in regions where few buoys are located, such as the Arctic and the western subpolar North Atlantic. Under extreme emission reductions, a strong and measurable (> 2 μatm) fingerprint signal begins to emerge at several of the buoy sites (Figure 3c). However, even at a subtropical site with low internal variance, such as the WHOTS buoy, and under the most extreme forcing scenario, the $\pm 1\sigma$ confidence interval of the fingerprint correlations encapsulates the zero correlation line (Figure 4b).

Detection of a COVID-related fingerprint in ΔpCO_2 from near real-time autonomous buoys is more likely when considering all 40 observational data streams simultaneously. Figure 4c reveals that, akin to the global-mean, the subsampled model ΔpCO_2 averaged across the 40 autonomous buoy locations has higher correlations with the fingerprint than that of a single buoy location. Yet, it is still statistically unlikely to detect the fingerprint from this subsampled mean unless there is a much larger emissions reduction than that which has been observed to date.

4 Conclusions and Discussion

We use an ensemble of Earth system model simulations to identify and assess the detectability of a COVID-related fingerprint in ΔpCO_2 and surface ocean pH. Our study reveals a unique fingerprint in modeled global mean ΔpCO_2 anomalies under COVID-like CO_2 emissions reductions due to the rapid slowdown and recovery of the emissions and the equilibration timescale for carbon in the upper mixed layer of the ocean. We find no discernible COVID fingerprint for modeled surface ocean pH, but rather a slight slowing of the continuous pH decline due to ocean acidification. A detection and attribution analysis conducted

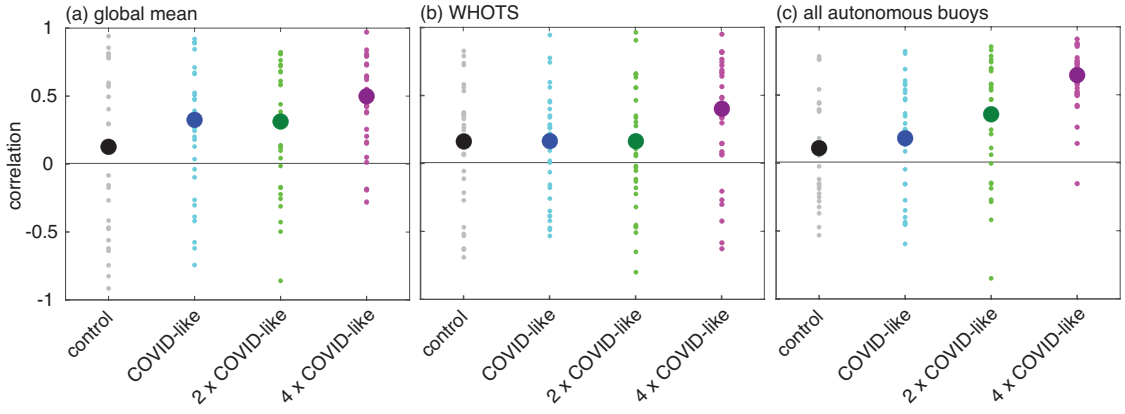

Figure 4. Detection and attribution of COVID-related fingerprints in ΔpCO_2 under four emission scenarios for (a) the modeled global-mean, (b) the WHOTS buoy location in the model, and (c) the mean of 40 autonomous buoy locations in the model, shown as the temporal correlation coefficients of individual ensemble members with the ensemble-mean fingerprint over 2019-2024. Small circles show the correlation coefficients from the 30 ensemble members, and the large circles show the mean correlation coefficients.

on individual model ensemble members shows that the ΔpCO_2 fingerprint is attributable to COVID emissions and potentially detectable in global-scale observations in cases with large emissions reductions. At local scales, however, observational detection is hampered by high internal variability.

Our results indicate that the detection of a COVID-related ΔpCO_2 fingerprint in future observations is more attainable from global-scale estimates, rather than regional or local measurements. While this is expected due to the low magnitude of internal variability at global scales and high variability at local scales [*Diffenbaugh et al.*, 2020; *Lovenduski et al.*, 2016], it nevertheless suggests that a large network of global-scale pCO_2^{oc} observations will be necessary to detect the COVID signal. Recent efforts to collect and process disparate pCO_2^{oc} data streams into a single cohesive database [e.g., *Sutton et al.*, 2019; *Bakker et al.*, 2016] will be highly useful for detection efforts. Even so, the ocean carbon community will continue to rely on observation-based, gap-filled surface ocean pCO_2 estimates to approximate the global-mean ΔpCO_2 and its temporal evolution. Continued improvement upon and testing of the reliability of these products is thus warranted [e.g., *Gloege et al.*, in review].

The COVID-related fingerprint in ΔpCO_2 is unique to the COVID-like emissions trajectory, permitting our investigation of detection and attribution. A more difficult task that awaits our community is the detection of a continuous emissions reduction in ocean carbon that may come about to support climate change mitigation policy. This detection will be further challenged by to the relatively high uncertainty in the global carbon cycle [*Peters et al.*, 2017]. Yet, it will become necessary to demonstrate the efficacy of emissions reductions on ocean carbon in the near future.

Acknowledgments

This research was supported by the National Science Foundation (OCE-1752724 and OCE-1948664). The authors' collaboration was facilitated in part by the Ocean Carbon and Biogeochemistry program through the Filling the Gaps in Observation-based Estimates of Air–sea Carbon Fluxes working group. The data from the CanESM5 simulations used in this study will be published through the Government of Canada Open Data Portal, and can be accessed at http://crd-data-donnees-rdc.ec.gc.ca/CCCMA/publications/COVID19/. We acknowledge the CCCma staff who contributed to producing these simulations. The WHOTS buoy air-

sea pCO_2 data are supported by the Office of Oceanic and Atmospheric Research of NOAA, U.S. Department of Commerce, including resources from the Global Ocean Monitoring and Observation program and are archived at https://doi.org/10.7289/V5DB8043. This is PMEL contribution 5189.

References

Bakker, D. C. E., B. Pfeil, C. S. Landa, N. Metzl, K. M. O'Brien, A. Olsen, K. Smith, C. Cosca, S. Harasawa, S. D. Jones, S.-I. Nakaoka, Y. Nojiri, U. Schuster, T. Steinhoff, C. Sweeney, T. Takahashi, B. Tilbrook, C. Wada, R. Wanninkhof, S. R. Alin, C. F. Balestrini, L. Barbero, N. R. Bates, A. A. Bianchi, F. Bonou, J. Boutin, Y. Bozec, E. F. Burger, W.-J. Cai, R. D. Castle, L. Chen, M. Chierici, K. Currie, W. Evans, C. Featherstone, R. A. Feely, A. Fransson, C. Goyet, N. Greenwood, L. Gregor, S. Hankin, N. J. Hardman-Mountford, J. Harlay, J. Hauck, M. Hoppema, M. P. Humphreys, C. W. Hunt, B. Huss, J. S. P. Ibánhez, T. Johannessen, R. Keeling, V. Kitidis, A. Körtzinger, A. Kozyr, E. Krasakopoulou, A. Kuwata, P. Landschützer, S. K. Lauvset, N. Lefèvre, C. Lo Monaco, A. Manke, J. T. Mathis, L. Merlivat, F. J. Millero, P. M. S. Monteiro, D. R. Munro, A. Murata, T. Newberger, A. M. Omar, T. Ono, K. Paterson, D. Pearce, D. Pierrot, L. L. Robbins, S. Saito, J. Salisbury, R. Schlitzer, B. Schneider, R. Schweitzer, R. Sieger, I. Skjelvan, K. F. Sullivan, S. C. Sutherland, A. J. Sutton, K. Tadokoro, M. Telszewski, M. Tuma, S. M. A. C. van Heuven, D. Vandemark, B. Ward, A. J. Watson, and S. Xu (2016), A multi-decade record of high-quality fCO_2 data in version 3 of the Surface Ocean CO_2 Atlas (SOCAT), *Earth Syst. Sci. Data*, *8*(2), 383–413, doi:10.5194/essd-8-383-2016.

Christian, J. R., V. K. Arora, G. J. Boer, C. L. Curry, K. Zahariev, K. L. Denman, G. M. Flato, W. G. Lee, W. J. Merryfield, N. T. Roulet, and J. F. Scinocca (2010), The global carbon cycle in the Canadian Earth System Model (CanESM1): Preindustrial control simulation, *J. Geophys. Res. Biogeosci.*, *115*(G3), doi:10.1029/2008JG000920.

Diffenbaugh, N. S., C. B. Field, E. A. Appel, I. L. Azevedo, D. D. Baldocchi, M. Burke, J. A. Burney, P. Ciais, S. J. Davis, A. M. Fiore, S. M. Fletcher, T. W. Hertel, D. E. Horton, S. M. Hsiang, R. B. Jackson, X. Jin, M. Levi, D. B. Lobell, G. A. McKinley, F. C. Moore, A. Montgomery, K. C. Nadeau, D. E. Pataki, J. T. Randerson, M. Reichstein, J. L. Schnell, S. I. Seneviratne, D. Singh, A. L. Steiner, and G. Wong-Parodi (2020), The COVID-19 lockdowns: a window into the Earth system, *Nat. Rev. Earth Environ.*, doi: 10.1038/s43017-020-0079-1.

Forster, P. M., H. I. Forster, M. J. Evans, M. J. Gidden, C. D. Jones, C. A. Keller, R. D. Lamboll, C. L. Quéré, J. Rogelj, D. Rosen, C.-F. Schleussner, T. B. Richardson, C. J. Smith, and S. T. Turnock (2020), Current and future global climate impacts resulting from COVID-19, *Nature Clim. Change*, doi:10.1038/s41558-020-0883-0.

Friedlingstein, P., M. O'Sullivan, M. W. Jones, R. M. Andrew, J. Hauck, A. Olsen, G. P. Peters, W. Peters, J. Pongratz, S. Sitch, C. Le Quéré, J. G. Canadell, P. Ciais, R. B. Jackson, S. Alin, L. E. O. C. Aragão, A. Arneth, V. Arora, N. R. Bates, M. Becker, A. Benoit-Cattin, H. C. Bittig, L. Bopp, S. Bultan, N. Chandra, F. Chevallier, L. P. Chini, W. Evans, L. Florentie, P. M. Forster, T. Gasser, M. Gehlen, D. Gilfillan, T. Gkritzalis, L. Gregor, N. Gruber, I. Harris, K. Hartung, V. Haverd, R. A. Houghton, T. Ilyina, A. K. Jain, E. Joetzjer, K. Kadono, E. Kato, V. Kitidis, J. I. Korsbakken, P. Landschützer, N. Lefèvre, A. Lenton, S. Lienert, Z. Liu, D. Lombardozzi, G. Marland, N. Metzl, D. R. Munro, J. E. M. S. Nabel, S.-I. Nakaoka, Y. Niwa, K. O'Brien, T. Ono, P. I. Palmer, D. Pierrot, B. Poulter, L. Resplandy, E. Robertson, C. Rödenbeck, J. Schwinger, R. Séférian, I. Skjelvan, A. J. P. Smith, A. J. Sutton, T. Tanhua, P. P. Tans, H. Tian, B. Tilbrook, G. van der Werf, N. Vuichard, A. P. Walker, R. Wanninkhof, A. J. Watson, D. Willis, A. J. Wiltshire, W. Yuan, X. Yue, and S. Zaehle (2020), Global Carbon Budget 2020, *Earth Syst. Sci. Data*, *12*(4), 3269–3340, doi:10.5194/essd-12-3269-2020.

Fyfe, J. C., V. V. Kharin, N. C. Swart, G. M. Flato, M. Sigmond, and N. P. Gillett (2020), Quantifying the influence of short-term emission reductions on climate, *Science Advances*, *in review*.

Gloege, L., G. A. McKinley, P. Landschützer, A. R. Fay, T. L. Frölicher, J. C. Fyfe, T. Ilyina, S. Jones, N. S. Lovenduski, C. Rödenbeck, K. B. Rodgers, S. Schlunegger, and Y. Takano (in review), Quantifying errors in observationally-based estimates of ocean carbon sink variability, *Global Biogeochem. Cycles*.

Gregor, L., and N. Gruber (2020), OceanSODA-ETHZ: A global gridded data set of the surface ocean carbonate system for seasonal to decadal studies of ocean acidification, *Earth Syst. Sci. Data*, *2020*, 1–42, doi:10.5194/essd-2020-300.

Landschützer, P., N. Gruber, and D. C. E. Bakker (2016), Decadal variations and trends of the global ocean carbon sink, *Global Biogeochem. Cycles*, *30*(10), 1396–1417, doi:10.1002/2015GB005359, 2015GB005359.

Landschützer, P., N. Gruber, and D. C. E. Bakker (2020), An observation-based global monthly gridded sea surface pCO_2 and air-sea CO_2 flux product from 1982 onward and its monthly climatology, (NCEI Accession 0160558), Version 5.5. NOAA National Centers for Environmental Information. Dataset.

Laughner, J. L., J. L. Neu, D. Schimel, P. O. Wennberg, K. Barsanti, K. Bowman, A. Chatterjee, B. Croes, H. Fitzmaurice, D. Henze, J. Kim, E. Kort, Z. Liu, K. Miyazaki, A. J. Turner, S. Anenberg, J. Avise, H. Cao, D. Crisp, J. de Gouw, A. Eldering, J. Fyfe, D. Goldberg, S. Hasheminassab, F. Hopkins, C. E. Ivey, N. S. Lovenduski, R. V. Martin, G. A. McKinley, L. Ott, B. Poulter, M. Ru, S. P. Sander, N. Swart, Y. L. Yung, Z.-C. Zeng, and the rest of the Keck Institute for Space Studies "COVID-19: Identifying unique opportunities for Earth system science" study team (in review), The 2020 COVID-19 pandemic and atmospheric composition: back to the future, *Proc. Nat. Acad. Sci.*

Le Quéré, C., R. B. Jackson, M. W. Jones, A. J. P. Smith, S. Abernethy, R. M. Andrew, A. J. De-Gol, D. R. Willis, Y. Shan, J. G. Canadell, P. Friedlingstein, F. Creutzig, and G. P. Peters (2020), Temporary reduction in daily global CO_2 emissions during the COVID-19 forced confinement, *Nature Clim. Change*, *10*(7), 647–653, doi:10.1038/s41558-020-0797-x.

Liu, Z., P. Ciais, Z. Deng, R. Lei, S. J. Davis, S. Feng, B. Zheng, D. Cui, X. Dou, B. Zhu, R. Guo, P. Ke, T. Sun, C. Lu, P. He, Y. Wang, X. Yue, Y. Wang, Y. Lei, H. Zhou, Z. Cai, Y. Wu, R. Guo, T. Han, J. Xue, O. Boucher, E. Boucher, F. Chevallier, K. Tanaka, Y. Wei, H. Zhong, C. Kang, N. Zhang, B. Chen, F. Xi, M. Liu, F.-M. Bréon, Y. Lu, Q. Zhang, D. Guan, P. Gong, D. M. Kammen, K. He, and H. J. Schellnhuber (2020), Near-real-time monitoring of global CO_2 emissions reveals the effects of the COVID-19 pandemic, *Nature Comm.*, *11*(1), 5172, doi:10.1038/s41467-020-18922-7.

Lovenduski, N. S., G. A. McKinley, A. R. Fay, K. Lindsay, and M. C. Long (2016), Partitioning uncertainty in ocean carbon uptake projections: Internal variability, emission scenario, and model structure, *Global Biogeochem. Cycles*, *30*(9), 1276–1287, doi:10.1002/2016GB005426, 2016GB005426.

McKinley, G. A., D. J. Pilcher, A. R. Fay, K. Lindsay, M. C. Long, and N. S. Lovenduski (2016), Timescales for detection of trends in the ocean carbon sink, *Nature*, *530*(7591), 469–472.

McKinley, G. A., A. R. Fay, Y. A. Eddebbar, L. Gloege, and N. S. Lovenduski (2020), External forcing explains recent decadal variability of the ocean carbon sink, *AGU Advances*, *1*(2), e2019AV000,149, doi:10.1029/2019AV000149.

Orr, J. C., R. G. Najjar, O. Aumont, L. Bopp, J. L. Bullister, G. Danabasoglu, S. C. Doney, J. P. Dunne, J.-C. Dutay, H. Graven, S. M. Griffies, J. G. John, F. Joos, I. Levin, K. Lindsay, R. J. Matear, G. A. McKinley, A. Mouchet, A. Oschlies, A. Romanou, R. Schlitzer, A. Tagliabue, T. Tanhua, and A. Yool (2017), Biogeochemical protocols and diagnostics for the CMIP6 Ocean Model Intercomparison Project (OMIP), *Geosci. Model Dev.*, *10*(6), 2169–2199, doi:10.5194/gmd-10-2169-2017.

Peters, G. P., C. Le Quéré, R. M. Andrew, J. G. Canadell, P. Friedlingstein, T. Ilyina, R. B. Jackson, F. Joos, J. I. Korsbakken, G. A. McKinley, S. Sitch, and P. Tans (2017), Towards real-time verification of CO_2 emissions, *Nature Clim. Change*, *7*(12), 848–850, doi:10.1038/s41558-017-0013-9.

Schlunegger, S., K. B. Rodgers, J. L. Sarmiento, T. L. Frölicher, J. P. Dunne, M. Ishii, and R. Slater (2019), Emergence of anthropogenic signals in the ocean carbon cycle, *Nature Clim. Change*, *9*(9), 719–725, doi:10.1038/s41558-019-0553-2.

Schlunegger, S., K. B. Rodgers, J. L. Sarmiento, T. Ilyina, J. P. Dunne, Y. Takano, J. R. Christian, M. C. Long, T. L. Frölicher, R. Slater, and F. Lehner (2020), Time of Emergence and Large Ensemble intercomparison for ocean biogeochemical trends, *Global Biogeochem. Cycles*, *34*(8), e2019GB006,453, doi:https://doi.org/10.1029/2019GB006453.

Sutton, A. J., R. A. Feely, S. Maenner-Jones, S. Musielwicz, J. Osborne, C. Dietrich, N. Monacci, J. Cross, R. Bott, A. Kozyr, A. J. Andersson, N. R. Bates, W.-J. Cai, M. F. Cronin, E. H. De Carlo, B. Hales, S. D. Howden, C. M. Lee, D. P. Manzello, M. J. McPhaden, M. Meléndez, J. B. Mickett, J. A. Newton, S. E. Noakes, J. H. Noh, S. R. Olafsdottir, J. E. Salisbury, U. Send, T. W. Trull, D. C. Vandemark, and R. A. Weller (2019), Autonomous seawater pCO_2 and pH time series from 40 surface buoys and the emergence of anthropogenic trends, *Earth Syst. Sci. Data*, *11*(1), 421–439, doi:10.5194/essd-11-421-2019.

Swart, N. C., J. N. S. Cole, V. V. Kharin, M. Lazare, J. F. Scinocca, N. P. Gillett, J. Anstey, V. Arora, J. R. Christian, S. Hanna, Y. Jiao, W. G. Lee, F. Majaess, O. A. Saenko, C. Seiler, C. Seinen, A. Shao, M. Sigmond, L. Solheim, K. von Salzen, D. Yang, and B. Winter (2019), The Canadian Earth System Model version 5 (CanESM5.0.3), *Geosci. Model Dev.*, *12*(11), 4823–4873, doi:10.5194/gmd-12-4823-2019.

World Meteorological Organization (2020), Can we see the impact of COVID-19 confinement measures on CO_2 levels in the atmosphere?, *WMO Greenhouse Gas Bulletin, number 16, 23 November 2020*.